IMPROVEMENTS IN PRECISION OF REAL-TIME PULSE HEIGHT ANALYSIS IN MICROCALORIMETER X-RAY DETECTORS

Stephen Thurgate[1,2] and Terrence Jach[2]

[1] Murdoch University, Perth, Australia

[2] National Institute of Standards & Technology, Gaithersburg, MD, USA

ABSTRACT

We analyze several pulse-height analysis schemes aimed at realizing maximum precision with TES (transition-edge sensor) microcalorimeter x-ray detectors. Issues of concern are nonstationary noise when the pulse takes the TES element into a higher resistance region, and variability of pulse shape with energy. Furthermore, system noise affects the precision analysis of pulse heights in two different ways: inaccuracy of the pulse height and variation in the triggering position on the pulse. We show that the weighted fitting of an entire pulse shape to obtain pulse height is an efficient way to obtain high resolution. We give a prescription for obtaining the best estimated pulse shape. A comparison is made between results with pulse shapes derived from different energy regions.

INTRODUCTION

Microcalorimeter x-ray detectors of different types have been employed in x-ray spectroscopy for a quarter of a century (Wollman *et al.*, 1997; Kenik *et al.*, 2004; Rodriguez *et al.*, 2008), but their use is still not widespread. The advantages of these detectors are high energy resolution and a wide energy range (Enss and McCammon, 2008). The disadvantages are a relatively low count rate per absorption element and the lack of a fixed energy scale. Nevertheless, improvements in performance, with the development of multiple detector elements and commercially reliable superconducting electronics, have completely transformed these detectors. Coupled with advances in the pulse-processing hardware and software, they can be seriously considered as a routine tool for energy-dispersive x-ray microanalysis (EDXMA) on electron microprobe instruments.

A microcalorimeter detector is simply an absorber of individual x-ray photons coupled to a temperature sensor. The most common type of sensor is the transition-edge sensor (TES), a thin superconducting film that is biased somewhere in the middle of the superconducting-normal phase transition (Irwin and Hilton, 2005). Very small changes in the temperature of the absorber lead to measurable changes in the resistance of the sensor, and the absorption of a single x-ray photon gives rise to a negative current pulse.

The ultimate limits in the precision of the detector energy resolution are determined by system noise, the nonlinearity of the TES, and the issue of pulse pileup. These factors also affect the count rates that can be achieved. Thus, the performance of the detector is really a question of

This document was presented at the Denver X-ray Conference (DXC) on Applications of X-ray Analysis.

Sponsored by the International Centre for Diffraction Data (ICDD).

This document is provided by ICDD in cooperation with the authors and presenters of the DXC for the express purpose of educating the scientific community.

Usage is restricted for the purposes of education and scientific research.

DXC Website
– www.dxcicdd.com

ICDD Website
- www.icdd.com

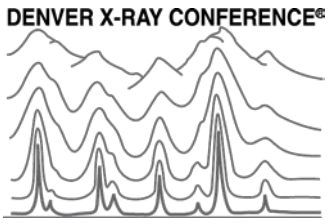

pulse processing. Microcalorimeter x-ray detectors are designed with absorbers suitable for a specific energy range E_r and are typically capable of resolution on the order of 5×10^{-4} of that range (Fowler *et al.,* 2016). In this paper we shall discuss the tradeoffs that have been employed to balance count rate and resolution. We propose an approach suited to real-time pulse processing which is likely to give the best resolution with practical count rates for use with scanning electron microscopes and electron microprobes.

CURRENT STATE OF PULSE MEASUREMENT METHODS

The characteristics discussed in this work apply to TES detectors designed for an energy range E_r of 200 eV to 10 keV, which is comparable to conventional silicon drift detectors used in microanalysis. A plot of our TES resistance as a function of bias voltage applied in a typical circuit (Lindeman *et al.*, 2004) is shown in Fig. 1. The TES is totally superconducting at zero bias and undergoes a gradual transition to a totally normal state with a resistance of approximately 6 mΩ at around 0.7 V bias. By choosing to operate at the bias point shown, X-ray photons heating the absorber will drive the TES further into the normal resistance region. Theoretical treatments of the equations governing the TES behavior show the amplitude of the current pulses saturating at increasing energy while their area increases (Cabrera, 2008).

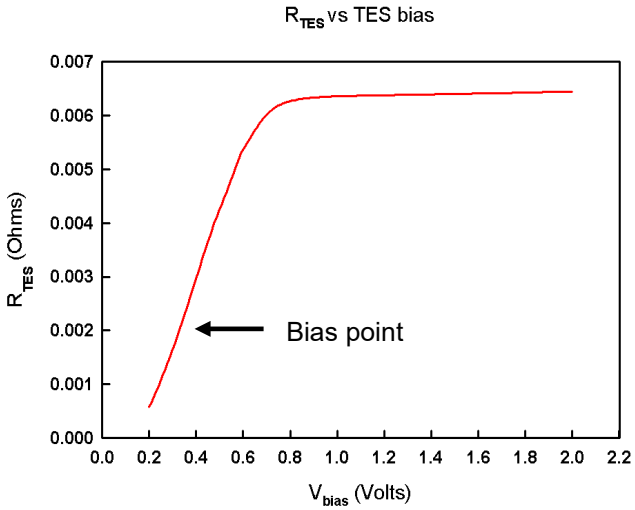

Figure 1. Plot of the resistance of a typical TES sensor as a function of a bias voltage showing the transition between the superconducting state (at $V_{bias} = 0$) and the totally normal state. The operating bias point is indicated.

A plot of the normalized pulse shape for the same TES detector is shown in Fig. 2 as a function of photon energy. It is seen that for incident photons up to approximately 7 or 8 keV energy, while the pulse amplitude may vary, the pulse shape remains relatively constant. Pulses due to photons beyond that energy are not only progressively nonlinear, but the noise spectrum becomes nonstationary. Successive noise and TES operating characteristics then depend on the previous values of the pulse. In the interest of operating over the maximum energy range possible, covariance matrix methods have been developed to extract pulse energies from pulse heights with the maximum resolution (Fixsen *et al.*, 2004; Fowler *et al.*, 2016). If each pulse is digitized over a time series of *n* samples, an *n x n* covariance matrix must be inverted after sufficient pulses are collected to ensure convergence. If the noise level is low, this can require

collecting a very large quantity of data, since the matrix will converge slowly. An optimal filter can be constructed from the covariance matrix and the model pulse shape using the method of least squares (Fixsen *et al*., 2014). The pulse height of any further pulses can be determined by application of this filter. If the pulse shape or noise distribution is changing rapidly with energy, a series of optimal filters must be fashioned to cover successive windows of energy.

Similar challenges to resolution arise over the issue of pulse pileup. The thermal relaxation inherent in microcalorimeter detectors leads to pulse rise times of the order of 10 μs and decay times of the order of 200 μs. Significant pulse pileup will result at even modest count rates of 100/s for a single detector element. In order to realize the resolution of 5 eV promised for the energy range specified above, pulse heights have to be accurately measured to 1 part in 2000. Methods devised to extract pileup pulses without forsaking energy resolution again require a covariance matrix approach, even when the noise is taken to be stationary (Fowler *et al.*, 2015).

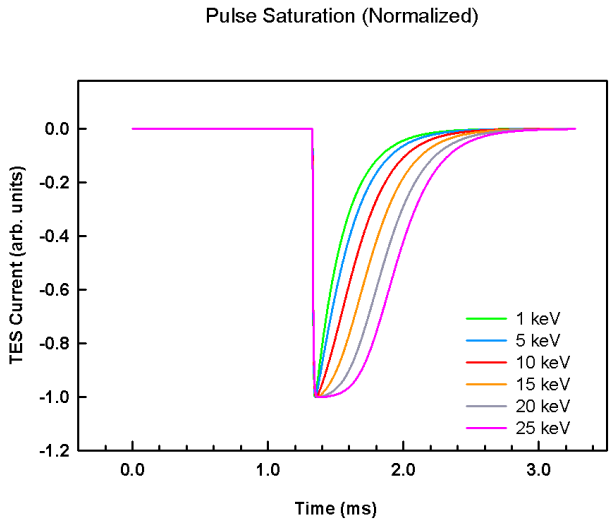

Figure 2. Calculated pulse shapes (normalized) as a function of incident photon energy for a representative TES detector, showing the nonlinear effect of saturation as the sensor goes increasingly normal.

DESCRIPTION OF PROPOSED MEASUREMENT METHOD

There are applications where operating the microcalorimeter TES detectors at the limits of energy range or count rate are highly desirable. In the interest of developing a pulse processing system that is sufficiently straightforward for use with EDXMA on electron microprobe instruments, a more conservative set of operating conditions can lead to a simplification of computation while achieving good energy resolution. We limit our energy range to approximately 75% of E_r (i.e., 7 keV-8 keV) and apply strong rejection of pileup pulses. Finally, we determine the optimal method to measure pulse heights under the constraints of stationary noise and discrete sampling. The method achieves an increased resolution compared to a conventional pulse height measurement while retaining the real-time counting performance. It also decreases the variation between detector elements.

Our procedure for the strong rejection of pileup pulses has been described previously (Jach and Thurgate, 2019; Thurgate and Jach, 2021). Briefly, a number of pulses whose amplitudes have

been digitized as time sequences is averaged to minimize the effects of pileup and noise. A second sequence of pulses, rejecting those with a low correlation coefficient with the previous average pulse, is then averaged in the same manner. This process is repeated multiple times, with successively tight correlation coefficients, to arrive at a "model pulse" that also has a stable, flat baseline. The final step is to record a sequence of pulses over the desired energy range with strong correlation to the model pulse, and to determine their pulse heights and areas. A polynomial fit to the ratio of pulse heights to pulse areas is used as the template for selecting pulses undistorted by pileup when obtaining actual spectra.

The pulse heights thus determined relied on polynomial fits to only the peak region of a pulse, calculated relative to the stable baseline. It was realized, however, that system noise affects the precision analysis of pulse heights in two different ways: inaccuracy of the pulse height and variation in the triggering position on the pulse. Once the pulse amplitude exceeds a threshold value, the pulse is digitized by a time sequence of samples. There are two components that relate to the trigger level. The random arrival of pulses relative to the fixed timing of digital sampling produces an ensemble of pulse displacements determined by Poisson statistics (Fowler *et al.*, 2016). In addition, amplitude noise on each pulse, Δv, in affecting the trigger level, results in an effective time offset of the leading edge of the pulse by an amount

$$\Delta t = \Delta v \left(\frac{dV(t)}{dt}\right)^{-1}, \quad (1)$$

where $dV(t)/dt$ is the slope of the pulse leading edge. These effects cause a variation in position of the actual maximum of the pulse, relative to the sampling points in the time sequence. They are responsible for a significant variation in the pulse height obtained by a polynomial fit to the peak, as determined from the digitized values.

This is readily seen by doing least squares fits of each entire pulse to the model pulse. The least squares method can be carried out very efficiently using the methods of linear algebra. In this case, let $a = (a_1, a_2, \dots, a_n)$ be the n discrete sampled values of the model pulse, and $b = (b_1, b_2, \dots, b_n)$ be the n discrete sampled values of any given pulse. Then the height x_1 and offset x_2 of each pulse can be fit by the matrix equation

$$Ax = b, \quad (2)$$

where

$$A = \begin{bmatrix} a_1 & 1 \\ a_2 & 1 \\ \cdot & \cdot \\ \cdot & \cdot \\ a_n & 1 \end{bmatrix}, \quad (3)$$

and

$$x = \begin{bmatrix} x_1 \\ x_2 \end{bmatrix} \quad . \quad (4)$$

The least squares solution is given by

$$A^T A x = A^T b\,, \quad (5)$$

leading to

$$x = (A^T A)^{-1} A^T b \, . \tag{6}$$

The variance of each point is given by

$$\sigma_i^2 = |b_i - a_i|^2 \, . \tag{7}$$

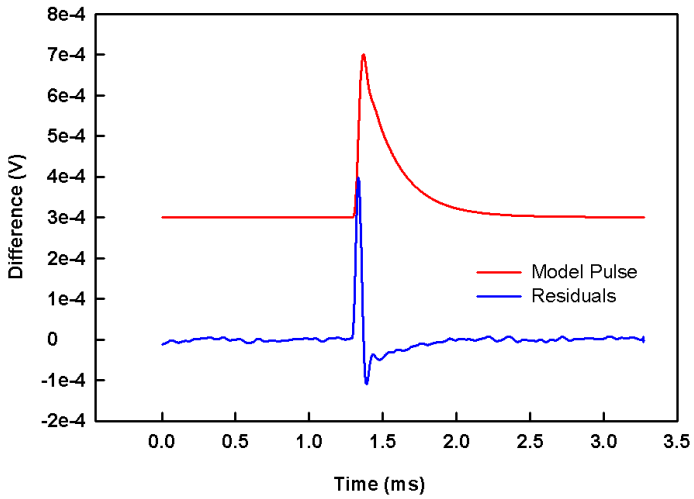

Figure 3. Plot of the residuals averaged over 25,000 pulses relative to the position of the model pulse (not to scale). The vertical scale describes the amplitude of the residuals assuming a model pulse height normalized to 1 V.

Fig. 3 shows the residuals at each sampled point in an individual pulse, as obtained in a least-squares fit to the model pulse, averaged over actual data from 25,000 pulses, and normalized to a pulse height of 1 V (the model pulse is shown for comparison). The least errors along the digitized values of the entire pulse are relatively uniform, except in the region of the leading edge and the peak of the pulse, where they are significantly greater. It suggests that the effective way to obtain a better estimate of pulse height is 1) to fit the entire pulse, instead of a polynomial approximation of the peak, and 2) to do a weighted fit which minimizes the effects of noise on triggering at the leading edge.

In that case, we weight each of the sampled points in a pulse by $w = (w_1, w_2, \ldots, w_n)$, and define a diagonal weighting matrix by $W_{mn} = w_m \delta_{mn}$

In that case, matrix equation (eqn. 2) is modified to

$$WAx = Wb, \tag{8}$$

And the least squares solution is given by

$$x = (A^T W^T W A)^{-1} A^T W^T W b \, . \tag{9}$$

Note that the least-squares fit is essentially a fit restricted to values along the main diagonal of the covariance matrix in the method cited previously (Fixsen *et al.*, 2004), so the computation is considerably simplified. Since the weighting matrix is diagonal, the addition of the weighting

matrix to the least squares fit of each pulse also has a minimal effect on the ability to do the calculations on each pulse from multiple detectors in real time.

While normally the weights are given by $w_i = (\sigma_i^2)^{-1}$, we employed a weighting matrix that imposed stricter constraints on the fitting process than usual. In the tail of the pulse, the standard deviation is the standard deviation of the errors relative to the model pulse once the individual pulses are normalized to 1. The weighting function in this region is defined as

$$w_i = 1 - \frac{\sigma_i}{S_i} \ , \tag{10}$$

where σ_i is the standard deviation of the i^{th} sample in the time series of the pulse, and S_i is the value of the model pulse at that time. The contribution to fitting any pulse to the model pulse decreases in the asymptotic value of the tail, and the weighting function becomes unreliable. At the point where S_i is less than 3 σ_i, we truncate the weighting function by setting $w_i = 1 - 0.333$.

To deal with the weight around the leading edge of the pulse, the maximum slope of the model pulse db/dt is calculated from the slope at the inflection point of the pulse. Individual phase delays are defined as the calculated value for the inflection point of each pulse relative to the trigger point. The standard deviation of all these phase delays σ_t is computed, and a standard deviation for the leading-edge height is assigned as

$$\sigma_{in} = \frac{db}{dt}\sigma_t \ , \tag{11}$$

with a weighting

$$w_{in} = 1 - \frac{\sigma_{in}}{S_{in}} \ , \tag{12}$$

where S_{in} is the value of the model pulse at the inflection point. Fig. 4 shows a plot of the weighting function relative to the model pulse.

Table I shows the improvement in resolution realized by an array of 8 TES detectors for the Si $K\alpha_{1,2}$ line excited by electrons in an SEM. The first column is the line width obtained using the polynomial fit to the peak of pulses to obtain the energy. The second column shows the line widths obtained by a weighted fitting of each entire pulse. The effect of fitting the entire pulse is to improve the average resolution by 12%. Furthermore, the standard deviation of resolutions from the ensemble of detectors improves by 33%. Thus, the effect of fitting the entire pulse brings the collective performance of the detectors into greater uniformity.

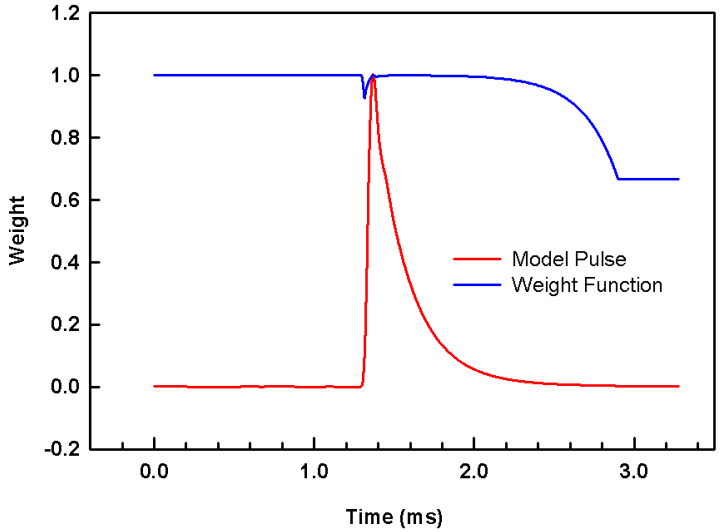

Figure 4. Plot of the weighting function determined by the residuals shown in Fig.3. The weights are scaled relative to the model pulse normalized to unity.

Table I

Detector	Old Resolution (eV)	New Resolution (eV)
A	5.18	4.55
B	5.32	4.58
C	5.45	4.72
D	5.10	4.55
E	5.71	4.93
F	5.12	4.60
G	4.68	4.24
H	5.10	4.41

A final question to be answered is whether the effect of adding pulses of different energies (and therefore slightly different lineshapes) to obtain the model pulse affects the overall resolution for the detector element. Fig. 5 shows the actual fit to the energy spectrum from a single detector element in the region of the Si $K\alpha_{1,2}$ line using a model pulse constructed from pulses of x-rays from all energies in the spectrum. To test the effect of pulse shape variation with energy, "model pulses" were then constructed not from data but generated from the characteristics of our TES detector elements (Cabrera, 2008) at two different energies. The same data were fitted using model pulses as they were calculated to look at the energy of the Si $K\alpha_{1,2}$ line (1740 eV) and the Fe $K\alpha_1$ line (6404 eV). After obtaining pulse energies by refitting the same data to the low energy "model pulse" and the high energy "model pulse", the width of the Si $K\alpha_{1,2}$ line obtained from the lower energy model pulse was 4.54 eV, and from the higher energy model pulse was 4.77 eV. Thus, for a detector limited in operation to 75% of its range of 10 keV, the effects of pulse nonlinearity have a minimal effect on the resolution.

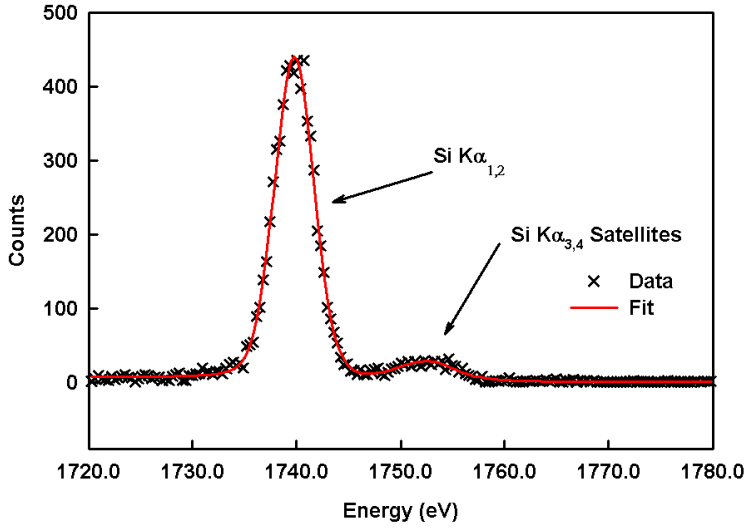

Figure 5. Plot of a fit to the Si $K\alpha_{1,2}$ line using the improved least squares solution detailed in Eq.9. The sensitivity to the energies used to determine the model pulse are described in the text.

CONCLUSIONS

We describe a system for extracting the energy of x-ray pulses from the TES microcalorimeter x-ray detector that provides superior energy resolution over simple pulse height analysis while proving computationally more economical that previously described covariant matrix methods. The weighted least-squares fitting of individual pulses to a model pulse in real time is easily accomplished and lends itself to high-resolution EDXMA detectors on an electron microprobe. The simplification is achieved at some cost of the ultimate detector energy range and by strict

rejection of pileup pulses, but incorporation of multiple detector elements make this less of an issue.

The system that we describe has been implemented in real-time operation with NI® ADC electronics and LabVIEW® software*. It has been operated with up to 16 detector elements at over 100 counts/s and could be extended to a larger number of elements. We believe that this represents a system that would be of practical value for EDXMA on electron microprobe instruments.

*Any mention of commercial products is for information only; it does not imply recommendation or endorsement by the National Institute of Standards and Technology.

ACKNOWLEDGEMENTS

The authors thank Blas Cabrera and Dale Fixsen for helpful discussions.

REFERENCES

Cabrera, B. (**2008**), "Introduction to TES Physics," J. Low Temp. Phys. 151, 82-93.

Enss, C. and McCammon, D. (**2008**). "Physical Principles of Low Temperature Detectors: Ultimate Performance Limits and Current Detector Capabilities," J. Low Temp. Phys. 151, 5-24.

Fixsen, D. J., Mosely, S. H., Cabrera, B., Figueoa-Feliciano, E. (**2004**). "Pulse estimation in nonlinear detectors with nonstationary noise," Nucl. Inst. Meth. Phys. Res. A 520, 555-558.

Fixsen, D. J., Mosely, S. H., Gerrits, T., Lita, A. E., and Nam, S. W. (**2014**). "Optimal Energy Measurement in Nonlinear Systems: An Application of Differential Geometry," J. Low Temp. Phys. 176, 16-26.

Fowler, J. W., *et al.* (**2015**). "Microcalorimeter Spectroscopy at High Pulse Rates: A Multi-Pulse Fitting Technique," Astrophys. Jour. Suppl. Ser. 219, 1-14.

Fowler, J. W., *et al.* (**2016**). "The Practice of Pulse Processing," J. Low Temp. Phys. 184, 374-381.

Irwin, K. D. and Hilton, G. C. (**2008**). "Transition-Edge Sensors," Topics Appl. Phys. 99, 63-149.

Jach, T. and Thurgate, S. M., (**2019**). US Patent. No. 10,245,249.

Kenik, E. A., Joy, D. C., and Redfern, D. (**2004**). "Microcalorimeter Detectors and Low Voltage SEM Microanalysis," Microchim. Acta 145, 81-85.

Lindeman, M. A. *et al.* (**2004**). "Impedance measurements and modeling of a transition-edge sensor calorimeter," Rev. Sci. Inst. 75, 1283-1289.

Rodriguez, M., Loidl, M., Leblanc, E., Bouchard, J., Fleischmann, A., and Enss, C. (**2008**). "Development of magnetic metallic calorimeters for X-ray metrology applications," X-ray Spectom. 37, 255-259.

Thurgate, S. and Jach, T. (**2021**). "Processing pulses from TES microcalorimeter X-ray detectors," Nucl. Inst. Meth. Phys. Res. A 1014, 165707.

Wollman, D. A., Irwin, K. D., Hilton, G.C., Dulcie, L. L., Newbury, D. E., and Martinis, J. M. (**1997**). "High-resolution energy-dispersive microcalorimeter spectrometer for X-ray microanalysis," J. Microsc. 188, 196-223.